Spheroidal nanoparticles as nanoantennas for fluorescence enhancement

A. Mohammadi*

Department of Physics,
Persian Gulf University,
75196 Bushehr, Iran
Fax: +98 771 454 1494
E-mail: mohammadi@pgu.ac.ir
*Corresponding author

F. Kaminski

Nano-Optics Group,
Laboratory of Physical Chemistry, ETH Zurich,
8093 Zurich, Switzerland
Fax: +41 633 1316

Presently at Niels Bohr Institute,
2100 Copenhagen, Denmark
E-mail: kaminski@nbi.dk

V. Sandoghdar and M. Agio

Nano-Optics Group,
Laboratory of Physical Chemistry, ETH Zurich,
8093 Zurich, Switzerland
Fax: +41 633 1316
E-mail: vahid.sandoghdar@ethz.ch
E-mail: mario.agio@phys.chem.ethz.ch

Abstract: Nanoantennas made of spheroidal metal nanoparticles are studied as a function of several parameters, namely aspect ratio, volume, background index and metal. Single nanospheroids are analysed using the polarisability theory with radiative and depolarisation corrections, while double spheroids are investigated using the finite-difference time-domain method. We focus on the spectral position of the plasmon resonance and on the scattering efficiency for applications related to the fluorescence enhancement of emitters. We show that a careful choice of the parameters allows covering wavelengths ranging from the UV to the near IR spectrum, while keeping the scattering efficiency close to 100%. We also discuss the role of the optical constants in determining the nanoantenna performances.

Keywords: nanoparticles; plasmon resonance; scattering; fluorescence; FDTD methods.

Reference to this paper should be made as follows: Mohammadi, A., Kaminski, F., Sandoghdar, V. and Agio, M. (2009) 'Spheroidal nanoparticles as nanoantennas for fluorescence enhancement', *Int. J. Nanotechnol.*, Vol. 6, Nos. 10/11, pp.902–914.

Biographical notes: Ahmad Mohammadi received the PhD Degree in Physics (2006) from Shiraz University, Iran, with a thesis on the improvements to the finite-difference time-domain (FDTD) method for applications in nano-optics and nano-photonics. From May 2005 to April 2006 he was visiting PhD student in the Nano-Optics group at ETH Zurich. He is currently Assistant Professor at the Persian Gulf University, Bushehr, Iran. His research interests focus on nano-optics, nano-photonics and computational electrodynamics using the FDTD method.

Franziska Kaminski studied Interdisciplinary Natural Sciences at ETH Zurich, where she also wrote her master thesis on three-dimensional FDTD simulations of plasmon resonances in gold nanoantennas. She is currently pursuing a PhD at the Niels Bohr Institute in Copenhagen, Denmark, studying the interface of ultra-cold atoms and light for quantum information physics.

Vahid Sandoghdar received the BS Degree in Physics from the University of California, Davis, and the PhD Degree in Atomic Physics from Yale University, New Haven, CT. He carried on research at the Ecole Normale Superieure, Paris, France, before moving to Konstanz, Germany, where he obtained the habilitation in Physics. Since 2001, he has been the Chair in Nano-Optics at ETH Zurich.

Mario Agio received the PhD Degree in Physics (2003) from the University of Pavia, Italy, with a thesis on the optical properties of semiconductor-based photonic crystals. He currently leads the theoretical efforts of the Nano-Optics group at ETH Zurich where he pursues the degree of habilitation. His research interests cover plasmonics, metamaterials, and the control of light-matter interaction using metal nanostructures.

1 Introduction

Metal nanoparticles hold great promise as systems for manipulating light and light-matter interaction at the nanoscale [1–4]. In particular, they are able to control the radiative decay rate of emitters placed in their near field [5–7]. These possibilities are based on the existence of a localised plasmon-polariton mode that allows establishing a Mie resonance even if the nanoparticle size is much smaller than the incident wavelength [8]. For these reasons such systems have been named nanoantennas [2]. Because metals absorb light in the optical domain, losses determine the nanoantenna performances and have to be taken into account in its design. For instance, we have recently shown that appropriate design rules lead to very large enhancements of the decay rate and the quantum efficiency of an emitter coupled to a gold nanoantenna [9]. Because these nanostructures have immediate application for improving light emission of dyes, nanocrystals and nanotubes, numerous experimental and theoretical works have been undertaken [10–17].

Gold and silver have been the materials of choice for making nanoantennas. However, having other suitable metals might offer more opportunities for applications, especially if technological issues are involved. For instance, recent works have been focusing on the spectroscopy of copper [18] and aluminium [19] nanostructures. In order to assess if these materials can be useful as nanoantennas, we have to investigate their optical properties, with emphasis on the spectral location of the plasmon resonance and on their absorption. A simple and straightforward approach is to look at the scattering cross section and at the scattering efficiency, respectively. The latter is defined as the ratio between the scattered and the extinguished powers, which gives an estimate of how much energy gets lost into absorption. However, we should keep in mind that a more precise assessment of the nanoantenna performances requires additional calculations [9,16,17].

We present analytical and numerical results on the cross sections of nanoantennas made of single and double nanospheroids for several parameters, including aspect ratio, volume, background index and metal. We choose nanospheroids because they have sufficient degrees of freedom to yield comprehensive information and at the same time represent a simple system. Moreover, they can be analytically treated using the dipolar approximation [8], which allows extensive parameter scans without much computational effort. They have been the model system for explaining the electromagnetic contribution to surface-enhanced Raman scattering (SERS) [20]. Indeed similar works, but focused on the near-field enhancement for SERS applications, are found in the literature [21,22].

2 Theory and numerical approach

R. Gans first studied the optical properties of silver nanospheroids within the electrostatic dipolar approximation [23]. Because the electrostatic polarisability does not account for radiation losses, the theory cannot be used for nanoparticles where light scattering is comparable or larger than absorption. Radiation losses can be added to the dipolar polarisability by imposing the conservation of energy in the interaction process. Radiation damping not only has consequences on light scattering, but also on the ability of nanoparticles to enhance the near field [24]. When the nanoparticle begins to have dimensions comparable to the wavelength of the incident light, the polarisability theory has to be corrected to account for retardation in the nanoparticle depolarisation [25]. With these improvements the dipolar approximation can be used to study the optical properties of single metal nanoparticles for a broad range of dimensions. Indeed, the theory has been extensively used for studying the near-field enhancement in SERS [22] and, more recently, the fluorescence enhancement of emitters coupled to metal nanoparticles [13,14].

For a prolate nanospheroid with a dielectric function ε, semi-major axis a and semi-minor axes b, embedded in a homogeneous medium having an index of refraction n_b, the dipolar polarisabilities read

$$\begin{aligned} \alpha_o &= 4\pi ab^2 \frac{\varepsilon-\varepsilon_\mathrm{b}}{3\varepsilon_\mathrm{b}+3L(\varepsilon-\varepsilon_\mathrm{b})}, \quad L=\frac{ab^2}{2}\int_0^\infty \frac{1}{(a^2+q)^{3/2}(b^2+q)}\mathrm{d}q \\ \alpha_{\mathrm{rad}} &= \frac{\alpha_o}{1-\dfrac{ik^3\alpha_o}{6\pi}}, \quad \alpha_{\mathrm{dep}} = \frac{\alpha_o}{1-\dfrac{ik^3\alpha_o}{6\pi}-\dfrac{k^2\alpha_o}{4\pi a}\left\{1-\dfrac{k^2a^2}{10}\right\}}, \end{aligned} \tag{1}$$

where L is the geometrical factor [8], $\varepsilon_b = n_b^2$, and α_o, α_{rad}, and α_{dep} are, respectively, the electrostatic, with radiative damping and with radiative plus depolarisation corrections dipolar polarisabilities. Moreover, the polarisabilities assume that plane-wave illumination is oriented and polarised such that the electric field is parallel to the spheroid semi-major axis. For a given polarisability α, the scattering (SCS) and extinction (ECS) cross sections are simply given by [8]

$$\text{SCS} = \frac{k^4}{6\pi}|\alpha|^2, \quad \text{ECS} = k\,\text{Im}(\alpha). \tag{2}$$

The scattering efficiency is defined by the ratio SCS/ECS and represents the fraction of energy that has interacted with the nanoparticle and is scattered to the far field. Equations (1) and (2) can be used to obtain analytical results for single nanospheroids.

When the nanoantenna is composed by two or more nanoparticles, the dipolar polarisability theory encounters difficulties. First, more complicated geometries make the analytical calculation of the polarisability challenging and tedious. Second, despite the small size of the nanoparticles, the strongly inhomogeneous near field sets up multipolar interactions that are neglected in the dipolar approximation [26]. For these reasons it is more convenient to approach the problem using a numerical method. Here we choose the three-dimensional finite-difference time-domain (FDTD) technique [27]. An incident plane wave is excited using the total-scattered field formulation. The SCS is computed by integrating the Poynting vector over a closed surface in the scattered field region. Likewise, the absorption cross section (ACS) is given by integrating the Poynting vector over a closed surface in the total field region. The ECS is simply the sum of the SCS with the ACS. The computational domain is terminated using convolution perfectly matched layers [28]. Because the FDTD method operates in the time domain, the dispersive dielectric function of the nanospheroids has to be fitted with a dispersion model that has an analytical Fourier transform. A good fit over a broad spectral range is obtained by using a Drude-Lorentz dispersion formula [29]. Because metal nanospheroids have sharp curvatures and a large dielectric function, we need to use a spatial discretisation as small as 1 nm to obtained converged results.

3 Results and discussion

3.1 Single nanospheroids

We study single nanospheroids using the analytical approach based on the dipolar polarisability. That gives us the possibility of scanning several parameters to identify those that yield a plasmon resonance at the desired wavelength and a high scattering efficiency. Figure 1(b) shows the SCS and the scattering efficiency for a gold nanospheroid, dimensions $a = 45$ nm, $b = 18$ nm and background $n_b = 1.5$, see inset in Figure 1(c). The curves have been obtained using different methods for comparison, namely FDTD, dipolar approximation with only radiative and also with depolarisation corrections. For the analytical results we have used the tabulated values of the dielectric function from [30], see Figure 1(d). We notice that the dipole approximation with radiative and depolarisation terms exhibits the best agreement with FDTD. To check that the discrepancy between analytical and numerical results is not due to the dispersion

models employed for the dielectric function, we also plot the outcome of the dipolar approximation using the same dielectric function implemented in the FDTD calculations. We find that the difference due to the fit is negligible, as expected from the very good agreement between the experimental and the analytical curves of Figure 1(d). Interestingly, the error in the scattering efficiency is much smaller than that for the SCS, except around 600 nm, where there is a higher order resonance neglected in the dipolar approximation. Nevertheless, if we concentrate on the dipolar resonance, the polarisability theory yields reliable results and it can be used to perform extensive parameter scans. We also notice that the scattering efficiency drops at wavelengths below 650 nm, because of the presence of an interband absorption peak, see Figure 1(d). Therefore, it is difficult to achieve good nanoantenna performances below 600 nm using gold [16,17].

Figure 1(a) displays the scattering efficiency and the SCS for a copper nanospheroid having the same dimensions and embedding medium of the gold one in Figure 1(b). Again, we compare the FDTD result with the dipolar approximation and find good agreement. The plasmon resonances in Figure 1(a) and 1(b) are almost at the same wavelength. The reason is that copper and gold have similar optical constants, as one sees by comparing Figure 1(c) with Figure 1(d). The main difference is that copper exhibits larger losses than gold, as evidenced by a broader plasmon resonance. Thus, the scattering efficiency is smaller, but not too small to make this material unsuitable for nanoantenna applications. We point out that also for copper an interband transition [31] dramatically reduces the scattering efficiency at wavelengths shorter than 650 nm. If the optical constants of gold were taken from [31], the scattering efficiency would be lower due to a larger value of the imaginary part of the dielectric function.

Figure 1 Scattering efficiency (dashed curves) and scattering cross section (solid curves) of a copper (a) and gold (b) nanospheroid (a = 45 nm, b = 18 nm) in glass (n_b = 1.5) computed using the FDTD method and the polarisability theory. Real (dashed curves) and imaginary part (solid curves) of the dielectric function for copper (c) and gold (d). The experimental data are taken from [31] and [30] for copper and gold, respectively. The curves have been fitted using a Drude-Lorentz dispersion model [29]. Inset in (c): nanospheroid with semi-major a and semi-minor b axes (see online version for colours)

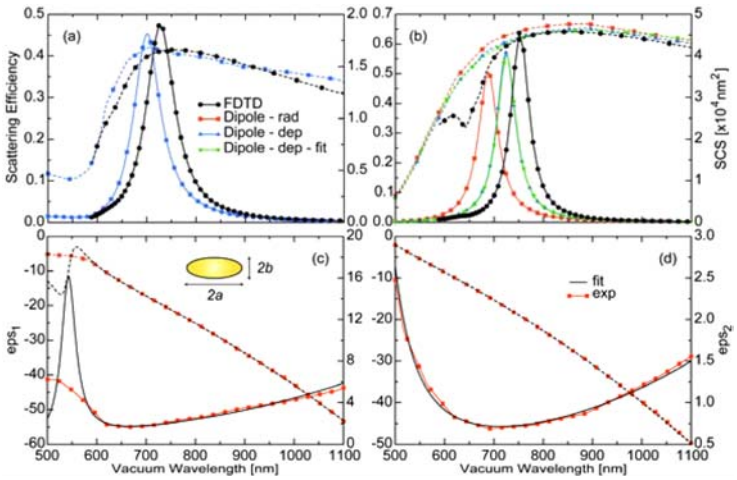

Figure 2(a) shows the scattering efficiency and the SCS of a spheroidal silver nanoparticle with dimensions and embedding medium like in the previous cases. The plasmon resonance is now shifted towards shorter wavelengths. Indeed, the optical constants of silver, see Figure 2(c), are similar to those of copper and gold, but with a higher plasma frequency [30]. Better results, however, are achieved if the experimental dielectric function is taken from [31]. Here the scattering efficiency and the SCS increase by a factor of two than compared to the previous situation. That exemplifies the importance of the actual values of the optical constants in a fabricated sample. To be conservative, we choose to work with the data having the largest imaginary part.

Figure 2 Scattering efficiency (dashed curves) and scattering cross section (solid curves) of a (a) silver and (b) aluminium nanospheroid (a = 45 nm, b = 18 nm) in glass (n_b = 1.5) computed using the FDTD method and the polarisability theory. Real (dashed curves) and imaginary part (solid curves) of the dielectric function for silver (c) and aluminium (d). The experimental data are taken from [30] and [31] (J&C) for silver, and from [32] for aluminium. The curves have been fitted using a Drude-Lorentz dispersion model [29] (see online version for colours)

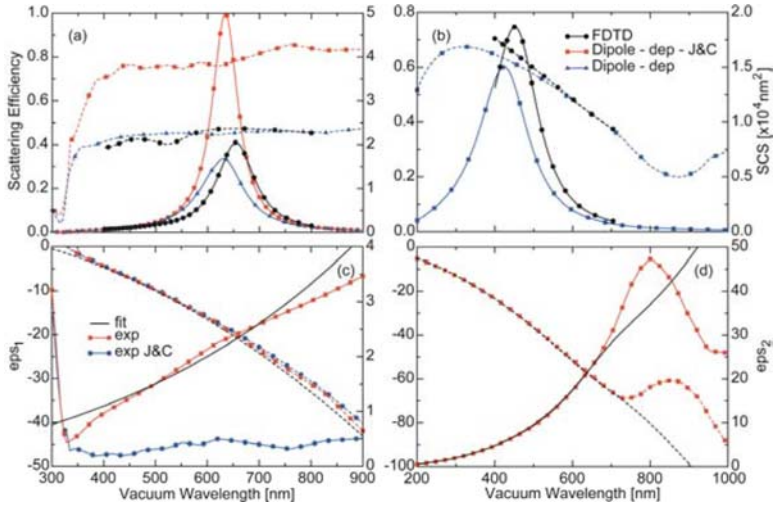

Figure 2(b) presents the result for a single nanospheroid made of aluminium, again with the same dimensions and background medium. The plasmon peak is further shifted towards the UV range, because aluminium exhibits an even higher plasma frequency than silver [32]. The scattering efficiency is close to 70% even if the imaginary part of the dielectric function is much larger than in the noble metals, see Figure 2(d). The result stems from the fact that the real part of the dielectric function is also very large. This reduces the penetration depth and thus absorption into the metal. Another important feature of aluminium is the interband transition located at 800 nm, which makes the scattering efficiency drop. Nevertheless, there is a broad spectral range between 200 nm and 600 nm where aluminium nanoantennas can replace silver, especially if the operating wavelength has to cover the UV spectrum.

In Figures 3–6 we summarise the outcome of the parameter scan for gold, copper, silver and aluminium nanospheroids, respectively. Panels (a), (c) and (e) display the wavelength of the plasmon resonance as a function of the semi-major and semi-minor axes. Panels (b), (d) and (f) give the scattering efficiency for the same wavelength.

Notice that we consider only prolate spheroids, hence $a > b$. Moreover, Panels (a) and (b) assume $n_b = 1.3$, (c) and (d) $n_b = 1.5$, and (e) and (f) $n_b = 1.7$. Figure 3 shows that the plasmon resonance shifts towards longer wavelength when the aspect ratio a/b increases, as expected from the polarisability theory. Concerning the scattering efficiency, the maximum is not reached for the largest volume, but rather for an aspect ratio of about 3–3.5 with $a = 60$–70 nm. As the background index increases, the plasmon resonance redshifts and the scattering efficiency increases, but the general trend is not changed. Figure 4 presents the same quantities for copper nanospheroids. As already discussed for Figure 1, the results are similar to those of gold, except that the scattering efficiency is lower.

Figure 5 is about silver nanospheroids. Again, the plasmon resonance shifts as a function of a and b similarly to gold and copper. However, the peak wavelength is about 200 nm less than for the previous materials because of the higher plasma frequency. The scattering efficiency is now maximal for a smaller aspect ratio than in Figures 3 and 4. Indeed we see that a/b should be about 1.7–2.3 for $a = 50$–70 nm. Notice also that the range is similar to that for gold, because for silver we have used the optical constants with the largest imaginary part [30]. Figure 6 reports the results for aluminium nanospheroids. Even if the plasmon resonance is located at wavelengths even shorter than for silver, the shift follows the same trend. On the other hand, the scattering efficiency is now larger for an aspect ratio close to one and for $a = 30$–40 nm. In fact higher aspect ratios and semi-major axes shift the plasmon resonance towards the spectral region where the interband transition occurs, thus reducing the scattering efficiency. Notice also that despite the strong imaginary part of the dielectric function, see Figure 2(d), the efficiency gets closer to 100% more than for nanospheroids made of the other materials.

Figure 3 Resonance wavelength, (a), (c) and (e), and scattering efficiency, (b), (d), and (f) for a gold nanospheroid in a background medium with $n_b = 1.3$, (a) and (b), $n_b = 1.5$, (c) and (d), and $n_b = 1.7$, (e) and (f) (see online version for colours)

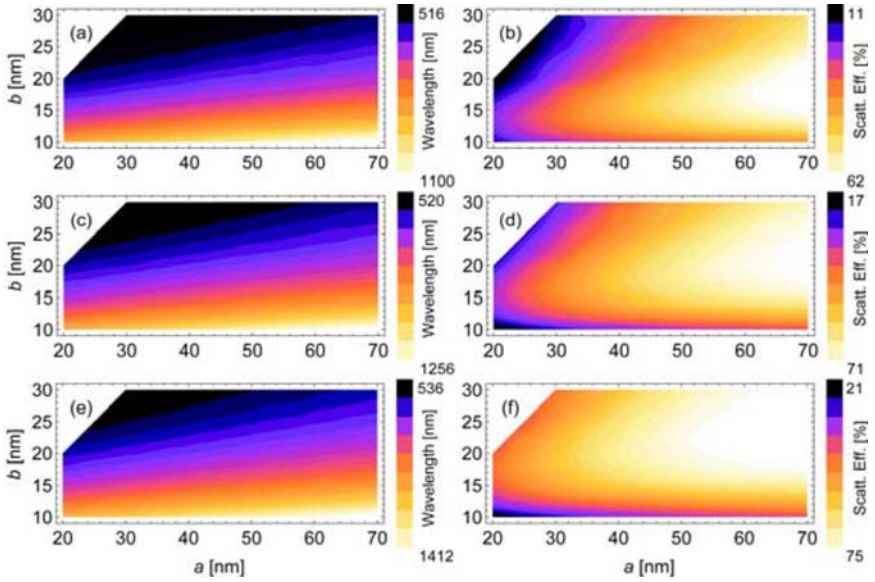

Figure 4 Resonance wavelength, (a), (c) and (e), and scattering efficiency, (b), (d), and (f) for a copper nanospheroid in a background medium with $n_b = 1.3$, (a) and (b), $n_b = 1.5$, (c) and (d), and $n_b = 1.7$, (e) and (f) (see online version for colours)

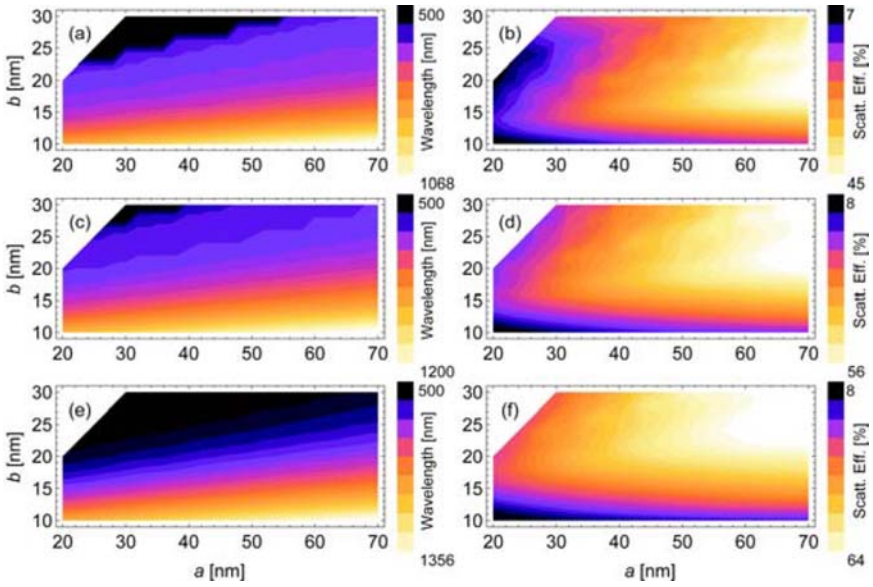

Figure 5 Resonance wavelength, (a), (c) and (e), and scattering efficiency, (b), (d), and (f) for a silver nanospheroid in a background medium with $n_b = 1.3$, (a) and (b), $n_b = 1.5$, (c) and (d), and $n_b = 1.7$, (e) and (f) (see online version for colours)

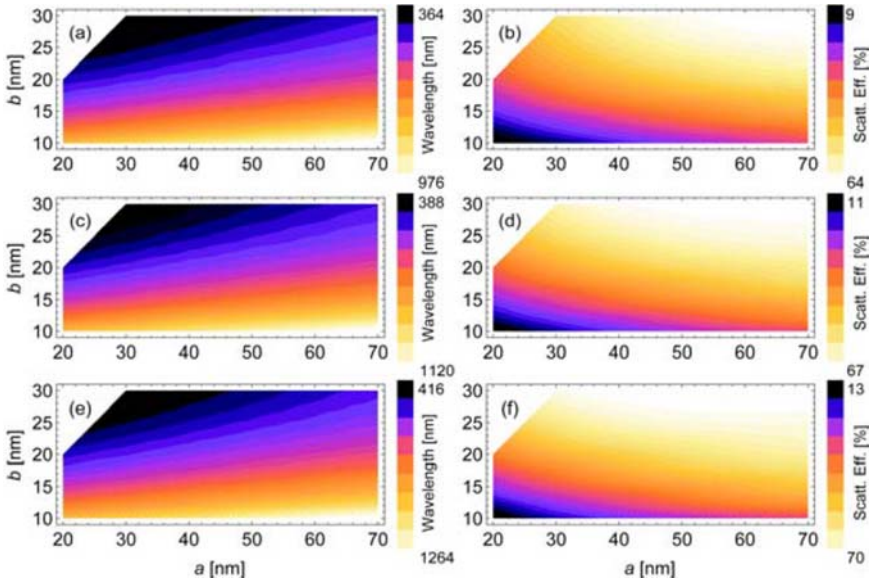

Figure 6 Resonance wavelength, (a), (c) and (e), and scattering efficiency, (b), (d), and (f) for an aluminium nanospheroid in a background medium with $n_b = 1.3$, (a) and (b), $n_b = 1.5$, (c) and (d), and $n_b = 1.7$, (e) and (f) (see online version for colours)

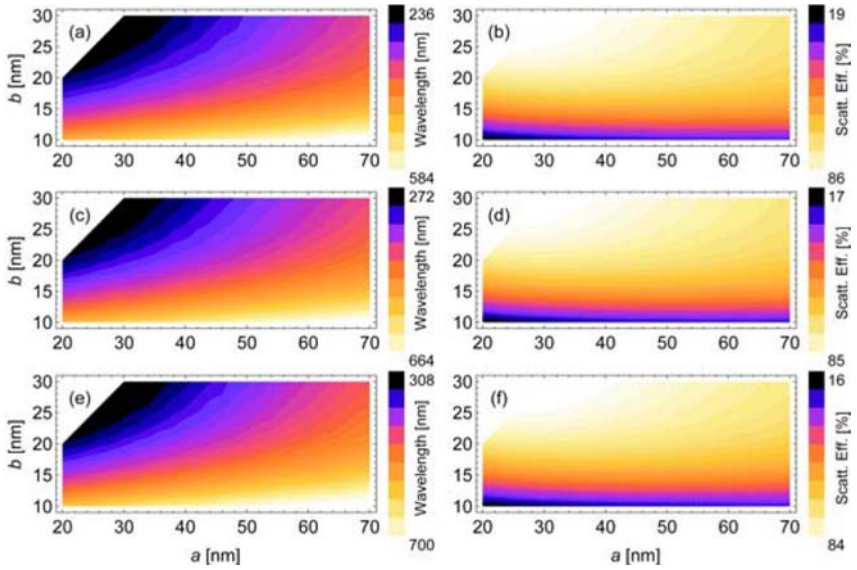

3.2 Double nanospheroids

Figures 3–6 show that by an appropriate choice of the nanospheroid parameters we can design nanoantennas with a large scattering efficiency ranging from the UV to the near IR spectrum. We already know that a nanoantenna composed by two nanospheroids yields a stronger near field [33] and a better quantum efficiency [9]. For this reason, we now consider pairs of nanospheroids and study the dependence of the plasmon resonance and of the scattering efficiency on parameters like aspect ratio, volume and interparticle distance. As already mentioned, because the two nanoparticles are very close to each other, to account for multipolar interactions we employ the FDTD method for the calculations.

Figure 7 shows the scattering efficiency and the SCS for two gold and copper nanospheroids embedded in glass ($n_b = 1.5$) as a function of the aspect ratio, with fixed separation $d = 20$ nm, see inset, and volume. As for the case of single spheroids, the plasmon resonance reshifts when the aspect ratio increases. Because we keep the volume constant, the scattering efficiency does not depend much on the aspect ratio. Nevertheless, in agreement with Figures 3 and 4, we notice that for gold the efficiency is maximal for a larger aspect ratio than copper. Moreover, in comparison with Figures 3(d) and 4(d), the scattering efficiency has increased, confirming that nanoantennas made of two nanospheroids are better than single ones. Notice also that a larger aspect ratio improves the SCS because the nanoparticles acquire a stronger dipole moment.

Figure 7 Scattering efficiency (dashed curves) and scattering cross section (solid curves) for two gold (a) and copper (b) nanospheroids in glass (n_b = 1.5) as a function of the nanoparticle aspect ratio a/b, with fixed separation d = 20 nm and volume: 1.6 (a = 38 nm, b = 24 nm), 2.4 (a = 50 nm, b = 21 nm) and 3.2 (a = 68 nm, b = 18 nm). Inset in (a): two nanospheroids (see online version for colours)

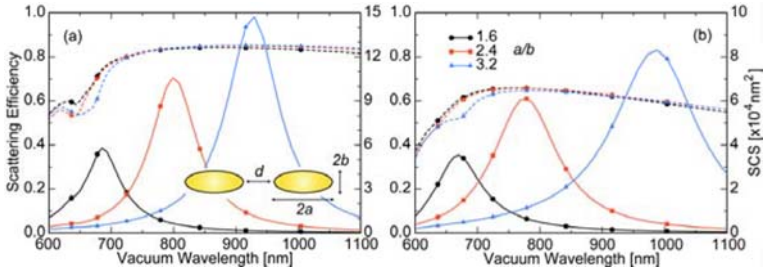

Figure 8 presents the scattering efficiency and the SCS for copper and silver as a function of the nanoparticle volume, with fixed separation d = 20 nm and aspect ratio a/b = 2.5. In agreement with Figure 4, the efficiency increases with the volume and, less pronounced, with the background index. Notice also that a larger volume redshifts and broadens the plasmon resonance because of radiative damping, which is proportional to the volume through α_o, see equation (1). The same occurs for silver, but at shorter wavelengths.

Figure 8 Scattering efficiency (dashed curves) and scattering cross section (solid curves) for two copper (a) and silver (b) nanospheroids in water (n_b = 1.3) and glass (n_b = 1.5) as a function of the nanoparticle volume, with fixed separation d = 20 nm and aspect ratio a/b = 2.5. The legend gives 2a times 2b in nm (see online version for colours)

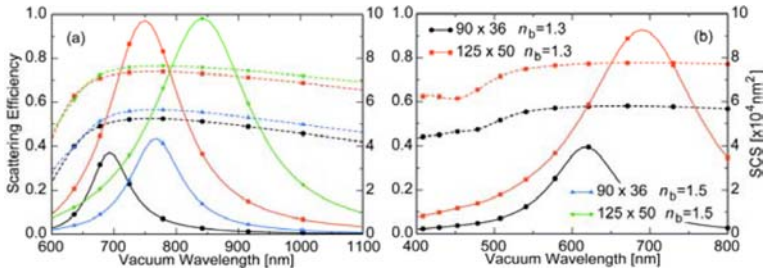

Figure 9 considers the effect of changing the particle separation on the plasmon resonance and compares the result to the case of a single nanospheroid. The materials are gold and aluminium and the other nanoantenna parameters are equal to those of Figures 1 and 2. Decreasing the distance redshifts the plasmon resonance, but it does not change appreciably the scattering efficiency. The latter increases because we have now two nanospheroids instead of one. Also the maximum value of the SCS does not depend much on the distance, while it is well known that the near field enhancement does [33]. Nevertheless, measuring the spectrum of the SCS provides accurate information on the particle distance [34]. The redshift caused by the plasmon interaction does not compromise the results found for single nanospheroids, that is, one can tune the parameters to obtain nanoantennas operating from the UV to the near IR spectral range. The advantage here is that the scattering efficiency is higher as well as the near field enhancement.

Figure 9 Scattering efficiency (dashed curves) and scattering cross section (solid curves) for two gold (a) and aluminium (b) nanospheroids (a = 45 nm, b = 18 nm) in glass (n_b = 1.5) as a function of the nanoparticle separation d (see online version for colours)

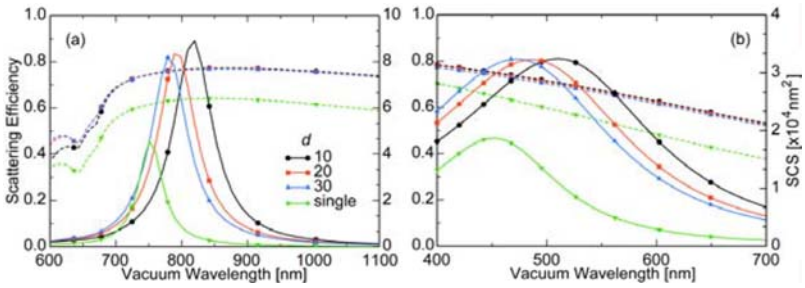

4 Conclusions

We have systematically studied the optical properties of nanoantennas made of one and two nanospheroids as a function of the aspect ratio, volume, background index and metal. Using the analytical method based on the polarisability theory, we have optimised the scattering efficiency and found the corresponding resonance wavelength. The scattering efficiency can be further improved by using two instead of one spheroid. However, one has to take into account the plasmon interaction that shifts and broadens the plasmon resonance. Moreover, these findings show that not only gold and silver are appropriate materials for plasmonic nanoantennas. Having at hand a choice of different metals provides more opportunity for the nanofabrication of devices, especially when the compatibility with existing technology is an important issue.

Choosing the right parameters allows to design nanoantennas with resonances ranging from the UV to the near IR spectra range, which cover several relevant emitters, including fluorescent dyes, nanocrystals and nanotubes [35–38]. Another important aspect that we have only mentioned here is the actual value of the optical constants of a nanoscale object. We have seen that the literature provides different results that have consequences on the nanoantenna design and performances. Therefore, the reliability and the reproducibility of the experimental dielectric function is an additional criterion for choosing the material for making the nanoantenna. The development of new fabrication methods [39] and the advancement in the experimental technique [40] can give a fundamental contribution on this topic.

Acknowledgements

We thank L. Rogobete, N. Mojarad, H. Eglidi and S. Götzinger for helpful discussions. A. Mohammadi is thankful to the Persian Gulf Univeristy Research Council for partial support. This work was financed by the ETH Zurich initiative on Composite Doped Metamaterials (CDM).

References

1 Meier, S. and Atwater, H.A. (2005) 'Plasmonics: localization and guiding of electromagnetic energy in metal/dielectric structures', *J. Appl. Phys.*, Vol. 98, No. 1, pp.011101-10.

2 Greffet, J.J. (2005) 'Nanoantennas for light emission', *Science*, Vol. 308, No. 5728, pp.1561–1563.

3 Van Hulst, N.F. (2007) 'Photonics: light in chains', *Nature,* Vol. 448, pp.141–142.

4 Danckwerts, M. and Novotny, L. (2007) 'Optical frequency mixing at coupled gold nanoparticles', *Phys. Rev. Lett.*, Vol. 98, pp.026104–4.

5 Ruppin, R. (1982) 'Decay of an excited molecule near a small metal sphere', *J. Chem. Phys.*, Vol. 76, No. 4, pp.1681–1684.

6 Anger, P., Bharadway, P. and Novotny, L. (2006) 'Enhancement and quenching of single-molecule fluorescence', *Phys. Rev. Lett.*, Vol. 96, pp.113002-4.

7 Kühn, S., Håkanson, U., Rogobete, L. and Sandoghdar, V. (2006) 'Enhancement of single-molecule fluorescence using a gold nanoparticle as an optical nanoantenna', *Phys. Rev. Lett.*, Vol. 97, pp.017402-4.

8 Bohren, C.F. and Huffman, D.R. (1983) *Absorption and Scattering of Light by Small Particles*, Wiley & Sons, New York.

9 Rogobete, L., Kaminski, F., Agio, M. and Sandoghdar, V. (2007) 'Design of plasmonic nanoantennae for enhancing spontaneous emission', *Opt. Lett.*, Vol. 32, No. 12, pp.1623–1625.

10 Lakowicz, J.R. (2005) 'Radiative decay engineering 5: metal-enhanced fluorescence and plasmon emission', *Anal. Biochem.*, Vol. 337, No. 2, pp.171–194.

11 Biteen, J.S., Pacifici, D., Lewis, N.S. and Atwater, H.A. (2005) 'Enhanced radiative emission rate and quantum efficiency in coupled silicon nanocrystals-nanostructured gold emitters', *Nano Lett.*, Vol. 5, No. 9, pp.1768–1773.

12 Mertens, H. and Polman, A. (2006) 'Plasmon-enhanced erbium luminescence', *Appl. Phys. Lett.*, Vol. 89, No. 21, pp.211107-3.

13 Mertens, H., Koenderink, A.F. and Polman, A. (2007) 'Plasmon-enhanced luminescence near noble-metal nanospheres: comparison of exact theory and an improved Gesten and Nitzan model', *Phys. Rev. B*, Vol. 76, pp.115123-12.

14 Mertens, H. and Polman, A. (2009) 'Strong luminescence quantum efficiency enhancement near prolate metal nanoparticles: dipolar versus higher-order modes', *J. Appl. Phys.*, Vol. 105, No. 4, pp.044302-8.

15 Bakker, R.M., Yuan, H-K., Liu, Z., Drachev, V.P., Kildishev, A.V., Shalaev, V.M., Pedersen, R.H., Gresillon, S. and Boltasseva, A. (2008) 'Enhanced localized fluorescence in plasmonic nanoantennae', *Appl. Phys. Lett.*, Vol. 92, No. 4, pp.043101-4.

16 Mohammadi, A., Sandoghdar, V. and Agio, M. (2008) 'Gold nanorods and nanospheroids for enhancing spontaneous emission', *New J. Phys.*, Vol. 10, pp.105015-14.

17 Mohammadi, A., Sandoghdar, V. and Agio, M. (2009) 'Gold, copper, silver and aluminium nanoantennas to enhance spontaneous emission', *J. Comput. Theor. Nanosci.*, in press.

18 Tilaki, R.M., Irajizad, A. and Mahdavi, S.M. (2007) 'Size, composition and optical properties of copper nanoparticles prepared by laser ablation in liquids', *Appl. Phys. A*, Vol. 88, pp.415–419.

19 Ekinci, Y., Solak, H.H. and David, C. (2007) 'Extraordinary optical transmission in the ultraviolet region through aluminum hole arrays', *Opt. Lett.*, Vol. 32, No. 2, pp.172–174.

20 Moskovits, M. (1985) 'Surface-enhanced spectroscopy', *Rev. Mod. Phys.*, Vol. 57, No. 3, pp.783–826.

21 Cline, M.P., Barber, P.W. and Chang, R.K. (1986) 'Surface-enhanced electric intensities on transition- and noble-metal spheroids', *J. Opt. Soc. Am. B*, Vol. 3, No. 1, pp.15–21.

22 Zeman, E.J. and Schatz, G.C. (1987) 'An accurate electromagnetic theory study of surface enhancement factors for Ag, Au, Cu, Li, Na, Al, Ga, In, Zn, and Cd', *J. Phys. Chem.*, Vol. 91, No. 3, pp.634–643.

23 Gans, R. (1915) 'Über die Form ultramikroskopischer Silberteilchen', *Ann. Phys.*, Vol. 47, pp.270–284.

24 Wokaun, A., Gordon, J.P. and Liao, P.F. (1982) 'Radiation damping in surface-enhanced raman scattering', *Phys. Rev. Lett.*, Vol. 48, No. 14, pp.957–960.

25 Meier, M. and Wokaun, A. (1983) 'Enhanced fields on large metal particles: dynamic depolarization', *Opt. Lett.*, Vol. 8, No. 11, pp.581–583.

26 Fuchs, R. and Claro, F. (1987) 'Multipolar response of small metallic spheres: nonlocal theory', *Phys. Rev. B*, Vol. 35, No. 8, pp.3722–3727.

27 Taflove, A. and Hagness, S.C. (2005) *Computational Electrodynamics: The Finite-difference Time-domain Method*, 3rd ed., Artech House, Norwood, MA.

28 Roden, A.J. and Gedney, S.D. (2000) 'Convolution PML (CPML): an efficient FDTD implementation of the CFS-PML for arbitrary media', *Microwave Opt. Technol. Lett.*, Vol. 27, No. 5, pp.334–339.

29 Kaminski, F., Sandoghdar, V. and Agio, M. (2007) 'Finite-difference time-domain modeling of decay rates in the near field of metal nanostructures', *J. Comput. Theor. Nanosci.*, Vol. 4, No. 3, pp.635–643.

30 Lide, D.R. (Ed.) (2006) *CRC Handbook of Chemistry and Physics*, 87th ed., CRC Press, Boca Raton, FL.

31 Johnson, P.B. and Christy, R.W. (1972) 'Optical constants of the noble metals', *Phys. Rev. B*, Vol. 6, No. 12, pp.4370–4379.

32 Palik, E.D. and Ghosh, G. (Eds.) (1998) *Handbook of Optical Constants of Solids*, Academic Press, San Diego, CA.

33 Aravind, P.K., Nitzan, A. and Metiu, H. (1981) 'The interaction between electromagnetic resonances and its role in spectroscopic studies off molecules adsorbed on colloidal particles or metal spheres', *Surf. Sci.*, Vol. 110, No. 1, pp.189–204.

34 Håkanson, U., Agio, M., Kühn, S., Rogobete, L., Kalkbrenner, T. and Sandoghdar, V. (2008) 'Coupling of plasmonic nanoparticles to their environments in the context of van der Waals-Casimir interactions', *Phys. Rev. B*, Vol. 77, pp.155408-9.

35 Bruchez, M., Moronne, M., Gin, P., Weiss, S. and Alivisatos, A.P. (1998) 'Semiconductor nanocrystals as fluorescent biological labels', *Science*, Vol. 281, No. 5385, pp.2013–2016.

36 Uppenbrink, J. and Clery, D. (1999) 'Single molecules', *Science*, Vol. 283, No. 5408, p.1667.

37 O'Connell, M.J., Bachilo, S.M., Huffman, C.B., Moore, V.C., Strano, M.S., Haroz, E.H., Rialon, K.L., Boul, P.J., Noon, W.H., Kittrell, C., Ma, J., Hauge, R.H., Weisman, R.B. and Smalley, R.E. (2002) 'Band gap fluorescence from individual single-walled carbon nanotubes', *Science*, Vol. 297, No. 5581, pp.593–596.

38 Ossicini, S., Pavesi, L. and Priolo, F. (2003) *Light-Emitting Silicon for Microphotonics*, Springer, Berlin.

39 Athanassiou, E.K., Grass, R.N. and Stark, W.J. (2006) 'Large-scale production of carbon-coated copper nanoparticles for sensor applications', *Nanotechnology*, Vol. 17, pp.1668–1673.

40 Stoller, P., Jacobsen, V. and Sandoghdar, V. (2006) 'Measurement of the complex dielectric constant of a single gold nanoparticle', *Opt. Lett.*, Vol. 31, No. 16, pp.2474–2476.